antioxidants

MDPI

Article

Tetrahydrocurcumin Attenuates $NaIO_3$-Induced Retinal Oxidative Injury via Suppression of NOX2-Derived ROS-Mediated Apoptosis

Tzu-Chun Chen [1,†], Thuy-Lan-Thi Vo [2,†], Shang-Chun Tsou [1], Hui-Min David Wang [3], Inga Wang [4], Chen-Ju Chuang [5], Hui-Wen Lin [1,6,*] and Yuan-Yen Chang [2,7,*]

1 Institute of Medicine, Chung Shan Medical University, Taichung 402, Taiwan
2 Department of Microbiology and Immunology, School of Medicine, Chung Shan Medical University, Taichung 402, Taiwan
3 Graduate Institute of Biomedical Engineering, National Chung Hsing University, Taichung 402, Taiwan
4 Rehabilitation Sciences & Technology, University of Wisconsin-Milwaukee, Milwaukee, WI 53211, USA
5 Emergency Department, St. Martin De Porres Hospital, Chiayi 600, Taiwan
6 Department of Medical Research, Chung Shan Medical University Hospital, Taichung 402, Taiwan
7 Clinical Laboratory, Chung Shan Medical University Hospital, Taichung 402, Taiwan
* Correspondence: d9138001@csmu.edu.tw (H.-W.L.); cyy0709@csmu.edu.tw (Y.-Y.C.)
† These authors have contributed equally to this work and share the first authorship.

Abstract

Oxidative stress is a major contributor to the development of age-related macular degeneration (AMD), and excessive oxidative stress can induce retinal pigment epithelium (RPE) dysfunction, apoptosis, and retinal degeneration. Nicotinamide adenine dinucleotide phosphate (NADPH) oxidase 2 (NOX2) is a major enzymatic source of reactive oxygen species (ROS); however, its mechanistic role in sodium iodate ($NaIO_3$)-induced oxidative injury remains unclear. Tetrahydrocurcumin (THC), the major metabolite of curcumin, exhibits potent antioxidant and cytoprotective activities, but its protective effects against AMD-associated retinal degeneration have not been fully elucidated. In the present study, we investigated whether THC protects against $NaIO_3$-induced ROS-mediated apoptosis in RPE cells through regulation of NOX2 signaling. *In vitro*, THC significantly attenuated $NaIO_3$-induced cytotoxicity and prevented apoptosis by suppressing hydrogen peroxide (H_2O_2) production and intracellular ROS accumulation in ARPE-19 cells. THC also preserved mitochondrial membrane potential by inhibiting the Src/$p47^{phox}$/NOX2 signaling pathway and subsequently attenuated mitochondria-mediated apoptotic signaling. Furthermore, THC markedly reduced the expression of apoptotic proteins, including Bax, cleaved caspase-3, and cleaved PARP, concomitantly with suppression of Ras/Raf/MEK/ERK signaling. Mechanistically, treatment with the selective NOX2 inhibitor GSK2795039 significantly attenuated $NaIO_3$-induced ROS accumulation and mitochondrial depolarization, while co-treatment with THC further enhanced these protective effects. *In vivo*, THC ameliorated $NaIO_3$-induced retinal structural abnormalities by preserving the outer nuclear layer (ONL), reducing caspase-3 expression, and improving pupillary light responses in mice. Collectively, these findings demonstrate that THC protects against $NaIO_3$-induced retinal degeneration through suppressing NOX2-dependent oxidative stress and downstream Ras/Raf/MEK/ERK-mediated apoptotic signaling, highlighting its potential as a therapeutic candidate for AMD and other oxidative stress-related retinal disorders.

Keywords: tetrahydrocurcumin (THC); age-related macular degeneration (AMD); $NaIO_3$; apoptosis; NOX2 and MEK/ERK signaling pathway

Check for updates

Academic Editors: Alessandra Napolitano, Francisco J. Romero and Jorge M. Barcia

Received: 8 April 2026
Revised: 30 May 2026
Accepted: 8 June 2026
Published: 18 June 2026

Copyright: © 2026 by the authors. Licensee MDPI, Basel, Switzerland. This article is an open access article distributed under the terms and conditions of the Creative Commons Attribution (CC BY) license.

1. Introduction

Age-related macular degeneration (AMD) is the leading cause of vision loss in individuals over 55 and affects 6–9% of the population worldwide. The number of AMD cases is expected to rise from 196 million in 2020 to 288 million by 2040 [1–3]. The annual incidence ranges from 0.3 per 1000 individuals aged 55–59 to 36.7 per 1000 in those aged 90 and older [2]. AMD is a neurodegenerative, multifactorial retinal disease influenced by aging, smoking, high-fat diets, light exposure, alcohol, genetic factors, and environmental pollution, all of which also increase the risk of other eye conditions such as dry eye disease, glaucoma, and cataracts, negatively impacting quality of life and health outcomes [4,5].

Previous studies suggest that oxidative stress and inflammation play key roles in AMD etiology [6–8]. Although excessive reactive oxygen species (ROS) accumulation can induce retinal pigment epithelium (RPE) cell death, the precise mechanisms underlying RPE degeneration in AMD remain incompletely understood. Previous studies have demonstrated that multiple forms of programmed cell death, including apoptosis and dysregulated autophagy, contribute to RPE loss [9,10]. Nicotinamide adenine dinucleotide phosphate (NADPH) oxidase 2 (NOX2) is another major source of ROS in addition to mitochondria [11,12]. Notably, the NOX family is unique among enzyme systems in that its primary biological function is the generation of ROS, including superoxide anion radicals ($O_2^{\bullet -}$) and hydrogen peroxide (H_2O_2). Studies have shown that NOX family members contribute to ROS overproduction, endoplasmic reticulum stress, autophagy, and apoptosis [13,14]. NOX2, also known as gp91^{phox}, consists of membrane-bound NOX2 and p22^{phox} subunits and the cytoplasmic subunit p47^{phox} and the small GTPase Rac [15,16]. Under oxidative stress conditions, p47^{phox} translocates from the cytoplasm to the membrane and interacts with membrane-associated catalytic components, resulting in NOX2 activation [17]. Previous studies have shown that NOX2 expression is relatively low in normal retinal tissues and retinal endothelial cells, but is overexpressed in pathological retinal conditions such as ischemic or diabetic retinopathy [18]. Our previous studies demonstrated that $NaIO_3$ induces ROS accumulation and activates caspase-dependent apoptotic signaling in RPE cells, ultimately contributing to retinal degeneration [7,19]. However, the mechanistic role of NOX2-derived oxidative stress in $NaIO_3$-induced RPE injury has not yet been fully elucidated. To date, no studies have investigated whether tetrahydrocurcumin (THC) protects against $NaIO_3$-induced retinal degeneration through modulation of NOX2-dependent oxidative stress signaling.

THC is the major metabolite of curcumin and exhibits relatively high stability under physiological conditions. Previous studies have demonstrated that THC possesses anti-inflammatory, hypoglycemic, hypolipidemic, and antioxidant activities [20,21]. THC has also been reported to provide neuroprotection against glutamate-induced neuronal cell death by inhibiting the accumulation of oxidative stress and phosphorylation of mitogen-activated protein kinases [MAPKs, including c-Jun N-terminal kinase (JNK), extracellular signal-regulated kinase (ERK), and p38] [22].

Interestingly, THC has been shown to attenuate obesity-induced skin damage by inhibiting NOX2, NOX4, and phosphorylated p65 expression, thereby reducing oxidative stress and inflammatory responses [23]. Furthermore, several studies have demonstrated that THC attenuates tissue damage by suppressing generation of ROS mediated through the MAPK pathway and NOX2 [24,25]. Therefore, the present study aimed to investigate the protective effects of THC against $NaIO_3$-induced retinal degeneration and to determine whether THC attenuates NOX2-mediated ROS accumulation, mitochondrial dysfunction, and Ras/Raf/MEK/ERK-dependent apoptosis signaling in RPE cells.

2. Methods

2.1. Cell Culture

The ARPE-19 cell line (ATCC, Manassas, VA, USA) [8,26] was cultured in Dulbecco's Modified Eagle Medium (DMEM; Cat# SH30022.02, GE Healthcare Life Sciences, HyClone Laboratories, Logan, UT, USA) supplemented with 10% heat-inactivated fetal bovine serum (FBS; Cat# 10437, Gibco, Thermo Fisher Scientific, Inc., Waltham, MA, USA), 100 µg/mL streptomycin, and 100 U/mL penicillin (Cat# 15140, Gibco, Waltham, MA, USA). Cells were maintained at 37 °C, 5% CO_2, with medium changes every 2 days.

2.2. MTT Assay

ARPE-19 cells were seeded in 12-well plates at a density of 2×10^5 cells/mL and pretreated with THC (0–50 µM) for 1.5 h. Subsequently, cells were incubated with or without $NaIO_3$ (6 mM; Sigma-Aldrich, St. Louis, MO, USA) for 24 h. Cell viability was assessed using the MTT assay as previously described by [27], with MTT-formazan measured at 570–655 nm using an ELISA plate reader (Tecan Sunrise, Tecan Austria GmbH, Salzburg, Austria).

2.3. Intracellular ROS and H_2O_2 Level Analysis

After treatment, cells were incubated for 1 h with 2 µM H2DCF-DA. The dye was then removed, and cells were collected with 0.25% trypsin-EDTA. ROS levels were measured using a FACSCalibur flow cytometer (BD Biosciences, San Jose, CA, USA) measuring green fluorescence (FITC, 530/30 nm). Data analysis was performed with CellQuest software (version 3.1), and experimental conditions and procedures were performed as previously described by [6]. Statistical values were normalized to 100% based on the control group (mock) and presented as percentage values in a bar graph. The supernatant was used for the H_2O_2 assay using a commercial kit (ab102500, abcam, Milpitas, CA, USA) according to the manufacturer's instructions. Absorbance was measured colorimetrically at 570 nm using an ELISA reader (Tecan Sunrise, Tecan Austria GmbH, Salzburg, Austria).

2.4. Mitochondrial Damage Assay

Mitochondrial damage was assessed using JC-1 staining (Cayman Chemical, Ann Arbor, MI, USA) and Hoechst 33342 (Invitrogen, Carlsbad, CA, USA), as described by [27].

2.5. Annexin V/PI Staining

To measure apoptosis levels, we applied Annexin V/propidium iodide dye (Annexin V-FITC Apoptosis Detection Kit, Enzo Life Sciences, Farmingdale, NY, USA) and imaged the samples using a FACSCalibur flow cytometer (BD Biosciences, CA, USA), following the method described by [6].

2.6. Western Blotting Assay

To assess the effects of THC on protein levels, Western blotting was performed using the following primary antibodies: cleaved-caspase-3 (sc-56053), Bax (sc-20067), Bcl-2 (sc-509), cleaved-PARP (sc-56196), K-RAS (sc-30), p-MEK1/2 (sc-81503), p-ERK1/2 (sc-31675), $p47^{phox}$ (sc-14015), β-actin (sc-47778), GAPDH (sc-32233) (all from Santa Cruz Biotechnology, Dallas, TX, USA), p-Src (D4964) and p-c-Raf (56A6) from Cell signaling (Danvers, MA, USA), and NOX2 (DF6520, Affinity Biosciences, Cincinnati, OH, USA). Bands were visualized with an ECL detection kit (Top Bio Corp, New Taipei, Taiwan) and quantified using EvolutionCapt software (v18.02, Vilber Lourmat SAS, F-77601 Marne-la-Vallée Cedex 3, France).

2.7. Animal Model Experiment

All animal protocols were conducted in accordance with [19] and adhered to the Institutional Animal Care and Use Committee (IACUC) guidelines of Chung Shan Medical University (IACUC no. 2680). BALB/c mice (6–8 weeks old, 28–29 g) were obtained from the National Laboratory Animal Center, Taiwan, and housed under standard conditions with a 12:12 h light cycle at 22 ± 3 °C. Mice were divided into three groups (n = 6 per group) and fed until 8 weeks old. Experimental groups received the following treatments:

Mock group: PBS 1× (200 μL, i.p.) on day 1, followed 2 h later by PBS (200 μL, i.v.), and then PBS 1× (200 μL, i.p.) daily from days 2–7.

$NaIO_3$ group: PBS 1× (200 μL, i.p.) on day 1, followed 2 h later by $NaIO_3$ (40 mg/kg, i.v.), and then PBS 1× (200 μL, i.p.) daily from days 2–7.

$NaIO_3$ + THC group: THC (25 mg/kg/day, i.p.) on day 1, followed 2 h later by $NaIO_3$ (40 mg/kg, i.v.), and then THC (25 mg/kg/day, i.p.) daily from days 2–7.

Mice were euthanized on day 7 using isoflurane (No. 08547, Panion and BF Biotech Inc., Taipei, Taiwan), and eyeball samples were collected for analysis to evaluate the effects of THC and/or $NaIO_3$.

2.8. Histopathology Assay

The effects of THC on retinal histology and imaging in mice were assessed as described in [6]. Mice eyeballs were collected, stained, and imaged. The entire retina, along with the inner nuclear layer (INL) and outer nuclear layer (ONL) thicknesses, was captured using an optical microscope (Olympus Optical, Tokyo, Japan). Measurements from six random areas were averaged for analysis. Cleaved-caspase-3 (clone 31A106, Santa Cruz Biotechnology, Santa Cruz, CA, USA) expression in the retina was evaluated using the BondMax automated staining system (Vision BioSystems Ltd., Newcastle Upon Tyne, UK).

2.9. Statistical Analysis

Data were presented as mean ± standard deviation (SD), with $n \geq 3$. One-way ANOVA was used to assess differences in both *in vitro* and *in vivo* experiments, followed by Duncan's post hoc test. A p-value < 0.05 was considered statistically significant. Different letters above the bars indicate significant differences between groups.

3. Results

3.1. THC Protects ARPE-19 Cells from $NaIO_3$-Induced Damage

To evaluate the cytotoxicity of THC in ARPE-19 cells, cells were pretreated with THC (0–100 μM) for 1.5 h and co-incubated with or without 6 mM $NaIO_3$ for 24 h. MTT assay results demonstrated that THC concentrations ≤50 μM did not significantly affect cell viability, whereas treatment with 100 μM THC markedly reduced cell survival, indicating concentration-dependent cytotoxicity at higher doses. Therefore, only non-cytotoxic concentrations (≤50 μM) were selected for subsequent experiments [Figure 1A, $p < 0.05$]. As shown in Figure 1B, $NaIO_3$ treatment reduced cell viability to less than 40%, while THC pretreatment markedly improved cell survival in a dose-dependent manner, demonstrating its protective effects against $NaIO_3$-induced retinal damage [Figure 1B, $p < 0.05$]. These findings indicate that THC effectively attenuates $NaIO_3$-induced cytotoxicity in ARPE-19 cells under non-toxic experimental conditions.

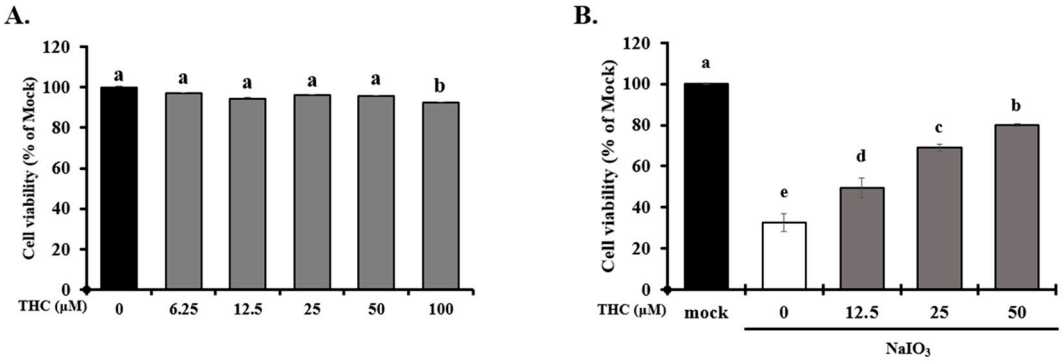

Figure 1. Effects of THC on cell survival in $NaIO_3$-induced ARPE-19 cells. ARPE-19 cells were pretreated with THC (0–100 μM) for 1.5 h, and subsequently incubated in the absence (**A**) or presence (**B**) of 6 mM $NaIO_3$ for 24 h. Cell viability was determined using the MTT assay, and absorbance was measured using a microplate reader. Data are presented as mean ± SD, n = 3, $p < 0.05$. Groups labeled with different letters (a–e) are significantly different from each other.

3.2. Effects of THC on Src-p47^{phox}-NOX2-Mediated ROS in $NaIO_3$-Induced ARPE-19 Cells

NOX enzymes play a specific role in ROS generation, and their dysregulation or overexpression contributes to various degenerative and hyperproliferative pathological conditions. Among them, NOX2-derived ROS represents a major source of oxidative stress, and its excessive accumulation can induce retinal injury [28]. Recent studies have shown that NOX2 reduces ROS levels and stress-induced ferroptosis, thereby protecting retinal ganglion cells [29].

In diabetic retinopathy, hyperglycemia activates NOX2 through upregulation of RAC1 and p47^{phox}, leading to increased cytoplasmic ROS production. This excessive ROS results in mitochondrial dysfunction and apoptosis, thereby contributing to disease progression [18].

To determine whether NOX2 is involved in $NaIO_3$-induced oxidative stress, we first examined NOX2 expression in ARPE-19 cells. As shown in Figure 2A, NOX2 expression increased in a dose-dependent manner when ARPE-19 cells were treated with different concentrations of $NaIO_3$ (2, 4, and 6 mM) for 18 and 24 h. Consistently, intracellular ROS levels were significantly elevated in $NaIO_3$-treated cells compared with untreated controls, also in a dose-dependent manner [Figure 2B]. Since ROS include both free radicals (such as superoxide and hydroxyl radicals) and non-radical species (such as H_2O_2), we further quantified H_2O_2 production using a commercial kit. As shown in Figure 2C, $NaIO_3$ treatment significantly increased H_2O_2 levels in a concentration- and time-dependent manner (2, 4, and 6 mM for 18 or 24 h).

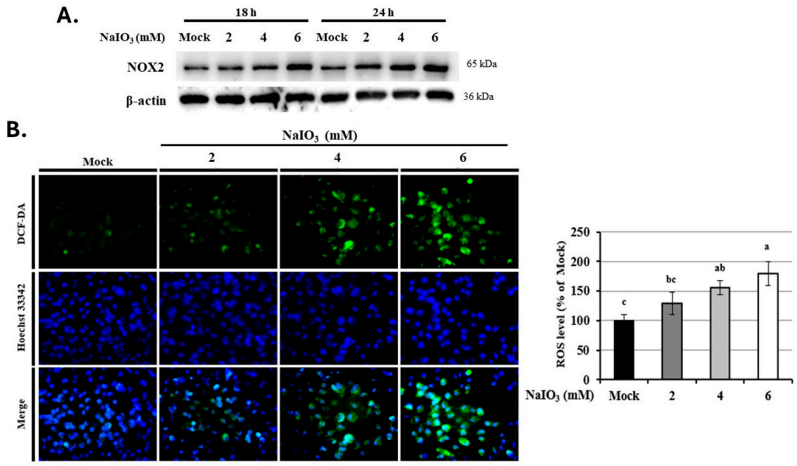

Figure 2. *Cont.*

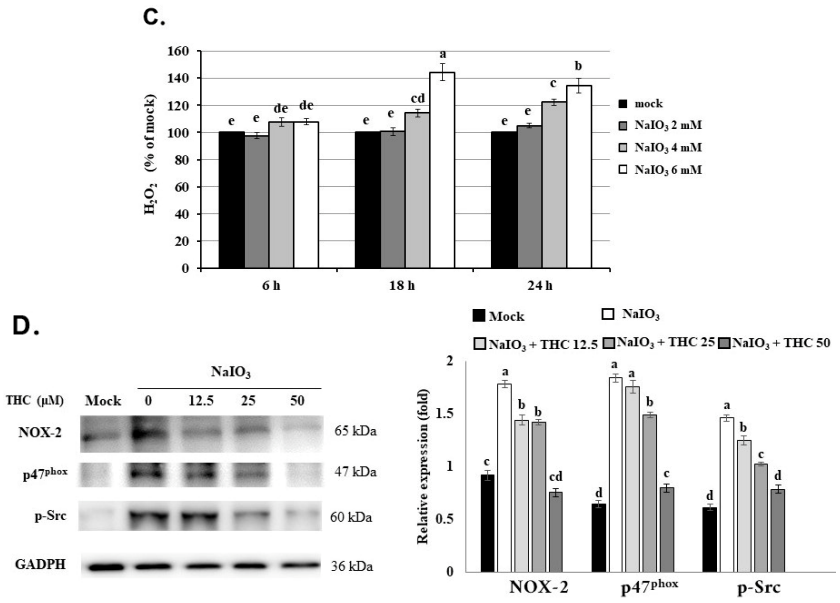

Figure 2. Effects of THC on Src-p47^{phox}-NOX2-mediated ROS in $NaIO_3$-induced ARPE-19 cells. ARPE-19 cells were pretreated without or with various concentrations of (0–50 μM) THC for 1.5 h, followed by incubation without or with different concentrations of $NaIO_3$ (0, 2, 4, and 6 mM) for 18 or 24 h. (**A**) NOX2 protein expression analyzed by Western blot. (**B**,**C**) Intracellular ROS levels and cellular H_2O_2 production measured using flow cytometry and ELISA, respectively. (**D**) Western blot and quantitative analysis showing the effects of THC on NOX2 expression, as well as the effects of p47^{phox} and phosphorylation Src-family proteins, in $NaIO_3$-treated ARPE-19 cells. Protein expression was quantified by densitometric analysis and normalized to β-actin or GAPDH as the loading control. Data are presented as mean ± SD, n ≥ 3, $p < 0.05$. Groups labeled with different letters (a–e) indicate statistically significant differences between them.

Previous studies have reported that Src plays an important role in the activation of NOX2 by inducing p47^{phox} expression in cell dysfunction [30,31]. To further investigate the regulatory role of NOX2 in $NaIO_3$-induced oxidative stress, we evaluated the effect of THC. As shown in Figure 2D, $NaIO_3$ exposure significantly increased NOX2 protein expression and induced the phosphorylation of its upstream signaling components, Src and p47^{phox}. Conversely, THC pretreatment markedly suppressed $NaIO_3$-induced NOX2 upregulation and inhibited the p47^{phox} and phosphorylation of Src. These results suggest that THC may inhibit $NaIO_3$-induced ROS generation by suppressing NOX2 activation through the downregulation of the Src/p47^{phox} pathway.

3.3. THC Reduces $NaIO_3$-Induced H_2O_2 Production and ROS Accumulation in ARPE-19 Cells

Oxidative stress resulting from excessive ROS accumulation in RPE cells is recognized as a key pathological mechanism contributing to AMD development [32]. Excessive ROS accumulation in the RPE damages organelles and promotes the formation of extracellular macular sclerosis-like deposits, thereby causing RPE functional decline, cell apoptosis, or the induction of autophagy or disorders [6,7,33]. To investigate the effects of THC on $NaIO_3$-induced oxidative stress, intracellular ROS levels were analyzed using DCFDA staining and flow cytometry, whereas H_2O_2 levels were measured using a commercial ELISA kit. As shown in Figure 3A, $NaIO_3$ treatment significantly increased intracellular ROS levels compared with the control group. Pretreatment with THC markedly reduced ROS accumulation in a concentration-dependent manner, and treatment with 25 and 50 μM THC restored ROS levels close to those observed in untreated cells ($p < 0.05$). Consistently, $NaIO_3$ exposure significantly increased H_2O_2 production, whereas THC pretreatment effectively suppressed H_2O_2 generation [Figure 3B].

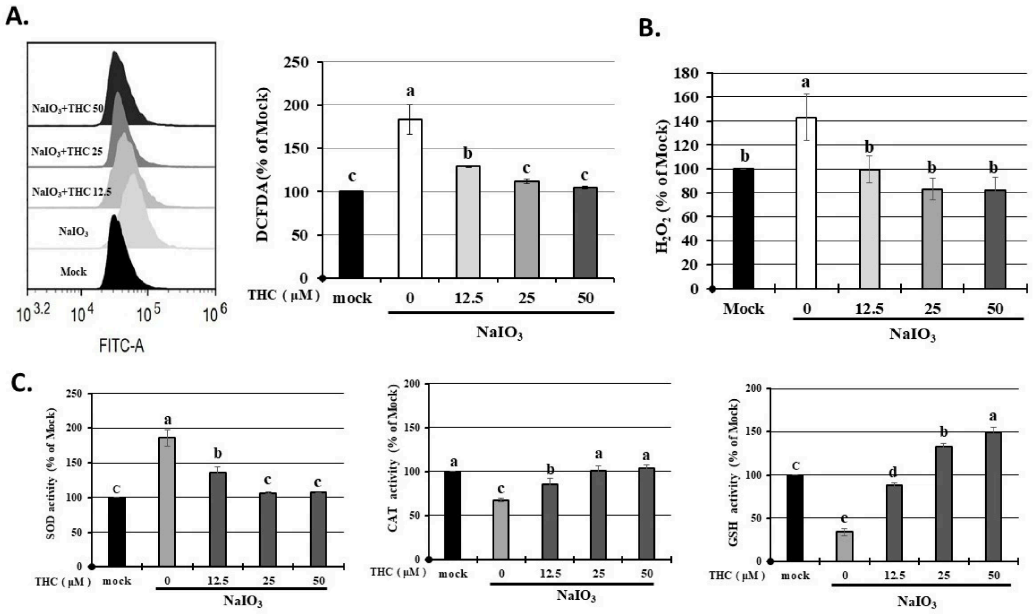

Figure 3. THC inhibits $NaIO_3$-induced H_2O_2 generation and thus reduces ROS accumulation in ARPE-19 cells. ARPE-19 cells were first treated with different concentrations of THC (0–50 μM) for 1.5 h and then co-treated with $NaIO_3$ for 18 h. (**A**) Intracellular ROS levels assessed by DCFDA staining and flow cytometry. (**B**) Cellular H_2O_2 production quantified by ELISA and (**C**) enzymatic activities of SOD and CAT, and intracellular levels of GSH in treated ARPE-19 cells, independently. Data are presented as the means ± SD of three independent experiments (n = 3). Different letters (a–e) in the statistical graphs indicate significant differences ($p < 0.05$) within each group.

To further determine whether THC modulates endogenous antioxidant defenses, the activities of antioxidant enzymes were examined. In physiological systems, cellular redox homeostasis is maintained through coordinated antioxidant systems, including superoxide dismutase (SOD), catalase (CAT), peroxidase (Prx), glutathione peroxidase (GPx), glutathione, vitamin C, and vitamin E [34]. As shown in Figure 3C, $NaIO_3$ treatment significantly increased SOD activity while reducing CAT and GSH activities. THC pretreatment markedly attenuated the $NaIO_3$-induced increase in SOD activity and restored CAT and GSH activities toward normal levels. Collectively, these findings indicate that THC effectively suppresses $NaIO_3$-induced oxidative stress by reducing ROS and H_2O_2 accumulation and by restoring antioxidant defense capacity in ARPE-19 cells. These results indicate that the increased H_2O_2 expression in the $NaIO_3$-induced group led to intracellular ROS accumulation, while THC pretreatment alleviated this phenomenon by inhibiting SOD activity and increasing CAT and GSH activities.

3.4. THC Attenuates NOX2-Dependent Oxidative Stress and Preserves Mitochondrial Function in $NaIO_3$-Treated ARPE-19 Cells

Mitochondria play critical roles in cellular metabolism, biosynthesis, ion homeostasis, and redox regulation, and are closely associated with aging, apoptosis, immune responses, and cell survival [35]. Previous studies have suggested that NOX2-derived ROS production represents an early upstream event that precedes mitochondrial ROS accumulation and subsequent mitochondrial dysfunction [36]. In particular, Kowluru et al. demonstrated that inhibition of NOX2 effectively attenuated mitochondrial damage and capillary cell apoptosis under oxidative stress conditions [36]. Therefore, we further investigated whether THC could protect mitochondrial integrity against $NaIO_3$-induced oxidative injury in ARPE-19 cells.

To evaluate mitochondrial membrane potential (ΔΨm), JC-1 staining was performed following $NaIO_3$ treatment. As shown in Figure 4A, exposure to $NaIO_3$ for 18 h markedly increased the accumulation of JC-1 monomers (green fluorescence), indicating mitochondrial depolarization and loss of mitochondrial function. In contrast, THC pretreatment significantly promoted the formation of JC-1 aggregates (red fluorescence), indicative of preserved mitochondrial membrane integrity, and this protective effect was enhanced in a dose-dependent manner. These findings suggest that THC effectively preserves mitochondrial function and protects against $NaIO_3$-induced oxidative mitochondrial injury in ARPE-19 cells.

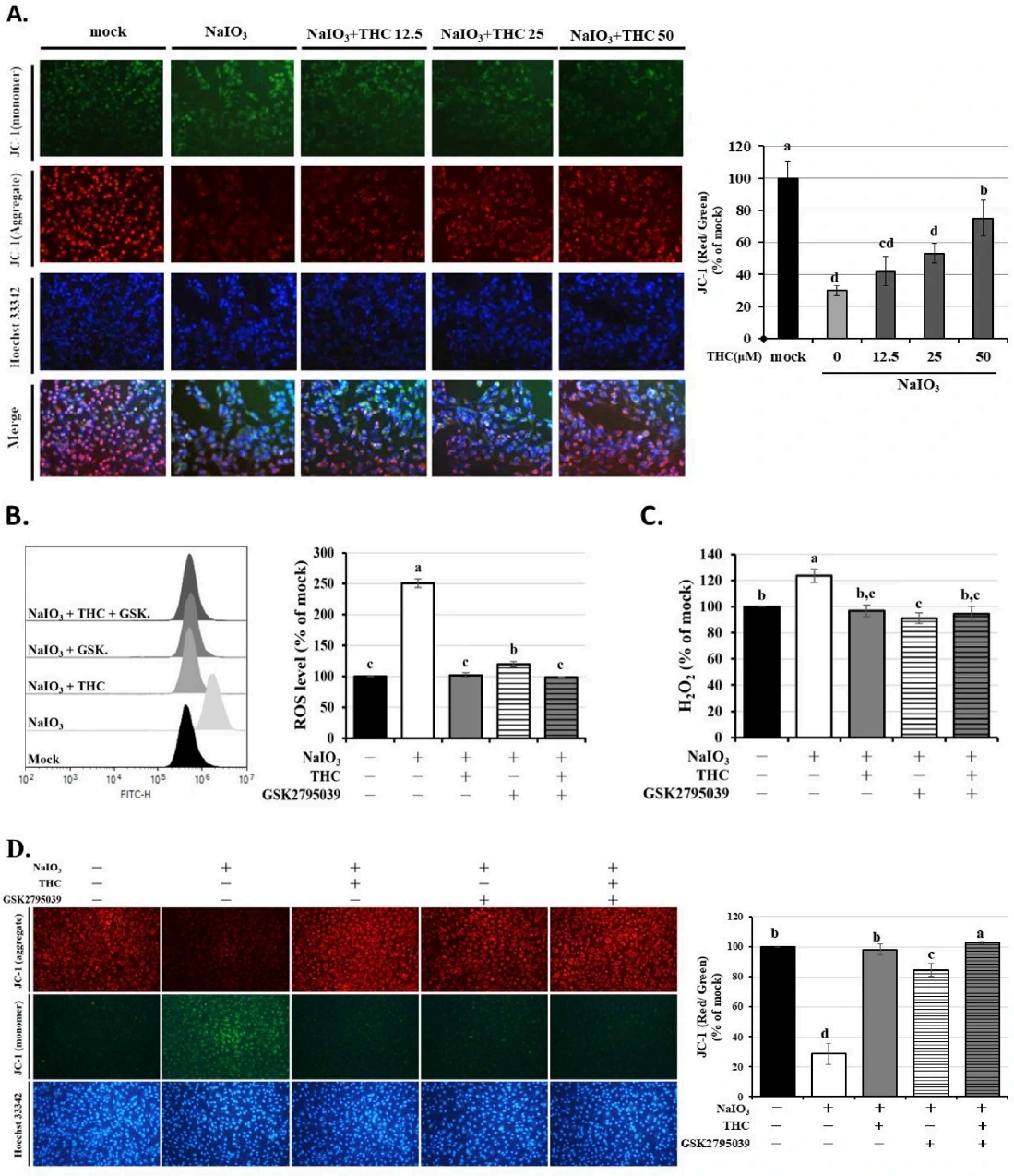

Figure 4. THC attenuates NOX2-dependent oxidative stress and mitochondrial dysfunction in $NaIO_3$-treated ARPE-19 cells. (**A**) ARPE-19 cells were pretreated with THC (0–50 μM) for 1.5 h and subsequently exposed to $NaIO_3$ for 18 h. Mitochondrial membrane potential (ΔΨm) was assessed by JC-1 staining. Red fluorescence indicates intact mitochondria, whereas green fluorescence indicates mitochondrial depolarization. (**B**) Intracellular ROS levels were measured by DCFDA staining and flow cytometry. (**C**) Extracellular H_2O_2 production was quantified using an ELISA-based assay. (**D**) Quantitative analysis of mitochondrial membrane potential based on the JC-1 red/green fluorescence

ratio. For mechanistic studies (**B**–**D**), ARPE-19 cells were pretreated with GSK2795039 (10 μM), THC (50 μM), or their combination for 1.5 h prior to $NaIO_3$ exposure. Data are presented as the means ± SD of three independent experiments (n = 3). Different letters (a–d) in the statistical graphs indicate significant differences ($p < 0.05$) within each group.

To further clarify whether $NaIO_3$-induced oxidative stress is mediated through NOX2 activation, we conducted additional mechanistic experiments using GSK2795039, a highly selective NOX2 inhibitor. ARPE-19 cells were pretreated with GSK2795039 alone or in combination with THC prior to $NaIO_3$ exposure, followed by analysis of intracellular ROS levels, H_2O_2 production, and mitochondrial membrane potential. Intracellular ROS generation was quantified using DCFDA fluorescence staining and flow cytometric analysis, whereas extracellular H_2O_2 levels were measured using an ELISA-based assay. As shown in Figure 4B, $NaIO_3$ treatment significantly increased intracellular ROS accumulation compared with the control group. Pretreatment with GSK2795039 markedly attenuated ROS production, while co-treatment with THC further suppressed ROS accumulation, providing direct pharmacological evidence that NOX2-derived ROS serves as a major upstream source of oxidative stress following $NaIO_3$ exposure. Similarly, $NaIO_3$ exposure significantly elevated H_2O_2 levels, whereas GSK2795039 pretreatment effectively reduced H_2O_2 production, and combined treatment with THC further enhanced this inhibitory effect (Figure 4C).

To determine whether NOX2-mediated oxidative stress contributes to mitochondrial dysfunction, mitochondrial membrane potential was further quantified using JC-1 fluorescence ratio analysis. As shown in Figure 4D, $NaIO_3$ treatment significantly reduced the red/green fluorescence ratio, indicating severe mitochondrial depolarization. Pretreatment with THC significantly restored mitochondrial membrane potential, whereas GSK2795039 alone also markedly attenuated mitochondrial dysfunction. Notably, combined treatment with GSK2795039 and THC exhibited superior protective efficacy in stabilizing mitochondrial membrane potential compared with GSK2795039 alone. Collectively, these findings suggest that NOX2-derived oxidative stress is a major upstream contributor to $NaIO_3$-induced mitochondrial dysfunction and that THC protects mitochondrial integrity, at least in part, through suppression of NOX2-dependent ROS generation and subsequent mitochondrial dysfunction.

3.5. THC Attenuates $NaIO_3$-Induced Apoptosis and Apoptosis-Related Protein Expression in ARPE-19 Cells

Previous studies have demonstrated that $NaIO_3$ induces apoptosis in ARPE-19 cells [6,7,19]. Therefore, we further investigated the mechanism by which THC alleviated $NaIO_3$-induced cell death. Annexin V-FITC/PI dual staining followed by flow cytometry was performed to quantify apoptotic cells, and Western blot analysis was employed to examine the expression of key apoptosis-related factors. As shown in Figure 5A, $NaIO_3$ treatment markedly induced apoptosis, elevating the apoptotic rate to approximately 34% of cells, compared to 7% in the mock group. THC pretreatment significantly attenuated this effect, reducing the apoptotic rate to around 23% in both the 12.5 and 25 μM THC-treated groups, with no significant difference observed between them. Notably, 50 μM THC further reduced the apoptotic population to 17% ($p < 0.05$).

As shown in Figure 5B, $NaIO_3$ treatment markedly increased the expression of apoptosis-related proteins such as cleaved-caspase-3, Bax, and cleaved-PARP compared with the control group. In contrast, pretreatment with THC significantly attenuated the expression of these apoptosis-related proteins. In terms of the performance of anti-apoptotic proteins, it was also found that $NaIO_3$ reduced Bcl-2 expression, while THC pretreatment

restored Bcl-2 levels. These findings indicate that THC protects ARPE-19 cells against $NaIO_3$-induced apoptosis by suppressing pro-apoptotic signaling and preserving anti-apoptotic protein expression.

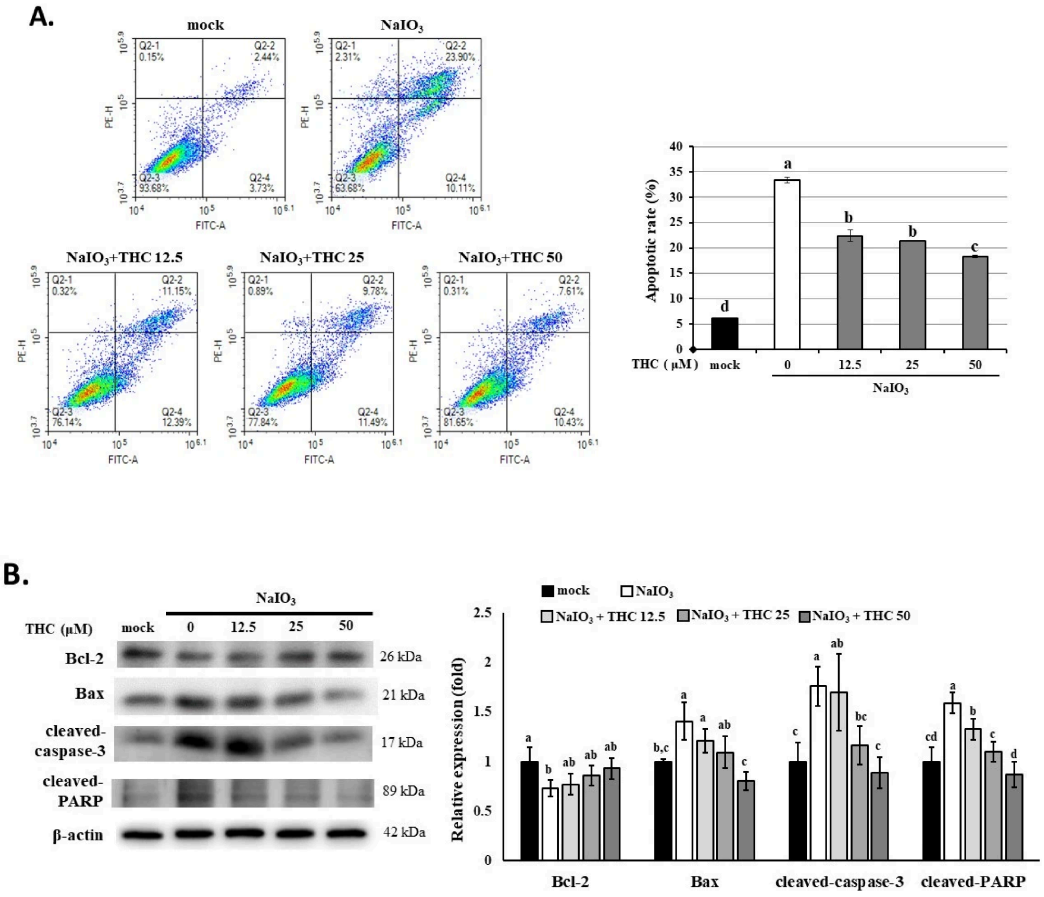

Figure 5. THC attenuates $NaIO_3$-induced apoptosis and expression of apoptosis-related proteins in ARPE-19 cells. The ARPE-19 cells were pretreated with different concentrations of THC (0–50 μM) for 1.5 h and then co-treated with $NaIO_3$ for 24 h. (**A**) Cell apoptosis was analyzed by Annexin V-FITC/propidium iodide (PI) staining and flow cytometry. (**B**) Expression levels of apoptosis-related proteins (Bcl-2, Bax, cleavage caspase 3, and cleavage PARP). Protein expression was quantified by densitometric analysis and normalized to β-actin as the loading control. Data are presented as the means ± SD of three independent experiments (n = 3). Different letters (a–d) in the statistical graphs indicate significant differences ($p < 0.05$) within each group.

3.6. THC Suppresses $NaIO_3$-Induced Activation of the Ras/Raf/MEK/ERK Signaling Pathway in ARPE-19 Cells

Recent studies have shown NOX2 activation through Src/extracellular signal-regulated kinase (ERK)-dependent pathway in neurodegeneration [37]. Studies have also shown that oxidized low-density lipoprotein activates NOX2 through the MAPK pathway to produce ROS, thereby inducing the formation of neutrophil extracellular traps [38]. Furthermore, Lee et al. reported that H_2O_2-mediated ERK1/2 activation is on Ras and Raf signaling, and can subsequently induce apoptotic cell death in mouse L929 cells [39]. These findings suggest that oxidative stress may act upstream of the Ras/Raf/MEK/ERK signaling cascade. Therefore, we further investigated whether activation of the Ras/Raf/MEK/ERK pathway contributes to the apoptosis in $NaIO_3$-treated ARPE-19 cells and whether THC can modulate this signaling cascade. As shown in Figure 6, $NaIO_3$ treatment significantly increased the expression of Ras and the phosphorylation levels of c-Raf, MEK1/2, and ERK1/2 compared with the control group. In contrast, pre-treatment with THC markedly suppressed the activation of these signaling molecules in

a dose-dependent manner. These findings indicate that THC attenuates $NaIO_3$-induced activation of the Ras/Raf/MEK/ERK pathway, which is associated with reduced oxidative stress, preservation of mitochondrial function, and suppression of apoptotic signaling in ARPE-19 cells.

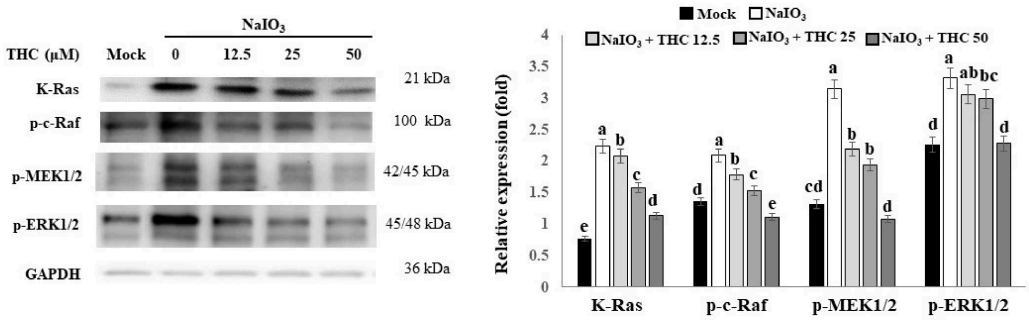

Figure 6. THC suppresses $NaIO_3$-induced activation of the Ras/Raf/MEK/ERK signaling pathway. The ARPE-19 cells were pretreated with different concentrations of THC (0–50 μM) for 1.5 h and then co-treated with $NaIO_3$ for 24 h. The protein levels of Ras, Raf, p-MEK, and p-ERK in ARPE-19 cells were analyzed by Western blotting. Protein expression was calculated from densitometry absorbance values of three separate experiments after they were corrected for GAPDH expression to obtain equal loading. Data are presented as the means ± SD of three independent experiments (n = 3). Different letters (a–e) in the statistical graphs indicate significant differences ($p < 0.05$) within each group.

3.7. THC Attenuates $NaIO_3$-Induced Retinal Degeneration and Functional Impairment in Mice

To determine whether THC protects against $NaIO_3$-induced retinal injury *in vivo*, retinal morphology, visual function, and apoptotic protein expression were evaluated in mice following daily THC administration. As shown in Figure 7A, hematoxylin and eosin (H&E) staining revealed that $NaIO_3$ treatment markedly disrupted retinal architecture, as evidenced by thinning of the outer nuclear layer (ONL), inner nuclear layer (INL), and photoreceptor inner/outer segments (ISs/OSs). In addition, accumulation of migratory cells and cellular debris, together with loss of normal retinal layer organization, was observed in $NaIO_3$-treated mice. In contrast, THC administration significantly attenuated these histopathological alterations and preserved retinal structural integrity.

To further evaluate retinal function, pupillary light reflex (PLR) analysis was performed [27,40]. As shown in Figure 7B, pupils from all experimental groups exhibited normal dilation under dark-adapted conditions. Following light stimulation, mice in the control group displayed rapid pupillary constriction, whereas $NaIO_3$-treated mice showed a markedly impaired constriction response, indicating retinal dysfunction. Notably, THC treatment partially restored pupillary constriction compared with the $NaIO_3$-treated group. Quantitative analysis further demonstrated that the percentage of pupil size after light exposure was significantly greater in the $NaIO_3$ group than in the control group, whereas THC treatment significantly improved this response, indicating preservation of retinal function.

Previous research results have also confirmed that $NaIO_3$ can induce apoptosis in RPE cells, so we also used an immunohistochemistry stain to detect caspase-3, a key marker of apoptosis. As shown in Figure 7C, $NaIO_3$ treatment markedly increased cleaved caspase-3 expression (indicated by red arrows) compared to the mock group. However, THC administration significantly reduced cleaved caspase-3 expression in retinal tissues. Taken together, these results suggest that THC attenuates $NaIO_3$-induced retinal degeneration, preserves retinal function, and suppresses apoptosis *in vivo*.

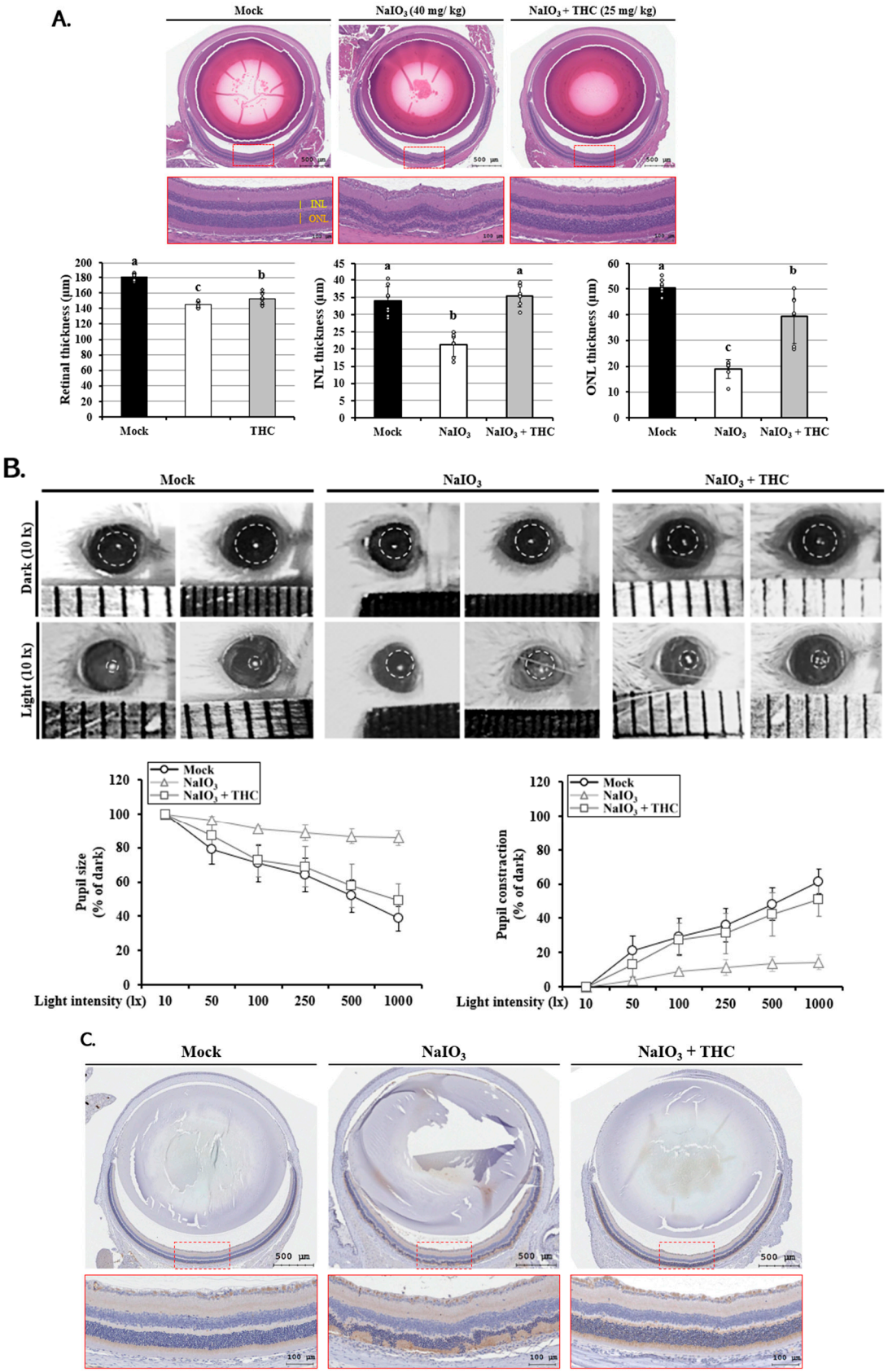

Figure 7. THC attenuates $NaIO_3$-induced retinal degeneration and functional impairment in mice. (**A**) H&E staining of retinas from the mock, $NaIO_3$-treated, and THC pretreatment + $NaIO_3$ groups. Quantitative analysis of total retinal, inner nuclear layer (INL), and outer nuclear layer (ONL) thickness is shown (n = 6 mice/group). (**B**) Assessment of retinal function by pupillary light reflex

(PLR) analysis. Representative images and quantitative analysis of pupil constriction responses following light stimulation are shown for the mock, $NaIO_3$-treated, and THC + $NaIO_3$ groups (n = 6 mice/group). (**C**) Immunohistochemical staining of apoptosis marker caspase 3 in retina tissues from the mock, $NaIO_3$-treated, and THC + $NaIO_3$ groups (n = 6 mice/group). Data are presented as the means ± SD of six independent experiments (n = 6). Different letters (a–c) in the statistical graphs indicate significant differences ($p < 0.05$) within each group.

4. Discussion

Retinal degeneration is generally regarded as a progressive and irreversible process driven by complex interactions between genetic susceptibility and environmental factors, which ultimately lead to RPE cell death and vision loss. Among them, AMD is the most common cause of retinal degeneration and can be classified into two major forms: dry AMD, characterized by RPE cell degeneration, and wet AMD, characterized by choroidal neovascularization [5]. In addition to genetic predisposition, environmental factors such as oxidative stress, inflammatory response, and hypoxia are also believed to be closely associated with retinal degeneration. In recent years, studies have shown that excessive accumulation of ROS within RPE cells plays a central role in the development and progression of dry AMD by promoting cellular dysfunction, mitochondrial damage, and cell death [33].

Oxidative stress leads to RPE cell death and is widely used as a disease model to recapitulate pathological processes associated with AMD. Consequently, $NaIO_3$-induced oxidative injury has been extensively used as an experimental model to mimic key pathological features of retinal degeneration and dry AMD [41,42]. In this study, we carefully selected THC concentrations to minimize inherent cytotoxicity while maintaining sufficient biological activity to assess its protective mechanisms under oxidative stress. The results showed that THC concentrations $\leq$ 50 μM had no significant effect on ARPE-19 cell viability, while 100 μM THC induced significant cytotoxicity, demonstrating a concentration-dependent biphasic effect. Therefore, subsequent experiments used only non-cytotoxic concentrations to ensure that the observed protective effects were not interfered with by direct toxic responses. Notably, THC pretreatment significantly restored cell viability after $NaIO_3$ treatment, accompanied by reduced ROS accumulation, maintenance of mitochondrial membrane potential, and inhibition of apoptosis signaling. These findings indicate that the selected THC treatment conditions provide a biologically responsive and therapeutically relevant window for studying oxidative stress-mediated retinal protection, without confounding effects from nonspecific toxicity.

Previous studies have demonstrated that members of the NADPH oxidase (NOX) family are important enzymatic sources of ROS and contribute to retinal injury in various ocular diseases, including choroidal neovascularization, oxygen-induced retinopathy, and diabetic retinopathy [43–45]. In human retinal endothelial cells, all known NOX isoforms, including NOX1–5 and DUOX1/2, have been identified and shown to participate in the regulation of retinal vascular homeostasis through ROS generation [44]. Under pathological conditions, dysregulated NOX activity results in excessive ROS production, leading to oxidative damage, mitochondrial dysfunction, and retinal neurodegeneration. However, the specific contribution of NOX2-mediated oxidative stress to $NaIO_3$-induced RPE injury has not been fully elucidated.

Our previous studies have shown that oxidative stress plays a key role in AMD, and $NaIO_3$ induces oxidative stress, apoptosis, and autophagy in RPE cells, leading to retinal dysfunction [7,19,46]. In the present study, $NaIO_3$ treatment markedly increased NOX2 expression, accompanied by elevated intracellular ROS accumulation and H_2O_2 production, ultimately resulting in ARPE-19 cell death (Figures 1 and 2). At the molecular level, we observed that exposure to $NaIO_3$ induced the phosphorylation of Src and $p47^{phox}$,

alongside the upregulation of NOX2 protein expression; however, pretreatment with THC significantly reduced the expression and activation of these proteins (Figure 2D). Furthermore, THC inhibited the production of H_2O_2 (Figure 3B) and subsequent excess ROS, thereby enhancing the cellular antioxidant defense capacity through the restoration of CAT and GSH activities (Figures 2 and 3).

To further clarify the precise mechanistic role of NOX2-mediated oxidative stress in mitochondrial dysfunction, we additionally employed GSK2795039, a highly selective NOX2 inhibitor, in combination with THC treatment. Consistent with previous reports demonstrating that NOX2-derived ROS acts upstream of mitochondrial oxidative injury, pharmacological inhibition of NOX2 by GSK2795039 significantly attenuated $NaIO_3$-induced intracellular ROS accumulation and H_2O_2 production, while simultaneously preserving mitochondrial membrane potential (Figure 4B–D). Notably, combined treatment with GSK2795039 and THC conferred greater protection than GSK2795039 alone, suggesting that THC-mediated retinal protection involves the suppression of NOX2-dependent oxidative stress in addition to complementary, parallel antioxidant mechanisms. These findings provide direct functional evidence supporting the concept that NOX2-derived ROS is a major upstream contributor to mitochondrial depolarization and subsequent apoptotic signaling during $NaIO_3$-induced retinal injury.

Ras signaling is known to play many cellular functions and can regulate cell proliferation, apoptosis, migration, fate determination, and differentiation by regulating downstream Raf kinase [47]. Accumulating evidence suggests that oxidative stress-mediated mitochondrial dysfunction is closely associated with activation of the Ras/Raf/MEK/ERK signaling cascade in retinal degeneration models. Previous studies demonstrated that H_2O_2-mediated ERK1/2 activation is Ras- and Raf-dependent and can directly induce apoptotic cell death [48], supporting the concept that oxidative stress acts upstream of the Ras/Raf/MEK/ERK apoptotic signaling pathway. In addition, previous retinal oxidative stress studies have shown that $NaIO_3$-induced apoptosis in ARPE-19 cells is mediated through activation of the MEK/ERK pathway, and pretreatment with selective MEK/ERK inhibitors, including U0126 and PD98059, significantly attenuated ROS-mediated apoptosis and mitochondrial dysfunction [6,46]. Furthermore, studies have demonstrated that curcumin-related compounds can modulate the Ras/Raf/MEK/ERK cascade under oxidative stress conditions [49].

Consistent with these previous findings, our results demonstrated that $NaIO_3$ exposure significantly increased the phosphorylation of Ras, Raf, MEK1/2, and ERK1/2, whereas THC pretreatment markedly suppressed the activation of this signaling cascade (Figure 6). Importantly, inhibition of Ras/Raf/MEK/ERK activation by THC occurred concomitantly with the suppression of ROS accumulation, preservation of mitochondrial membrane potential (Figure 4), and reduction of apoptotic signaling.

To further delineate the hierarchical relationship between the pathways evaluated in this study, our findings strongly suggest that the Src/$p47^{phox}$/NOX2 axis and the Ras/Raf/MEK/ERK cascade operate together within a unified upstream-downstream signaling network rather than as independent events. Specifically, $NaIO_3$ exposure drives the initial activation of the Src/$p47^{phox}$/NOX2 complex, culminating in a profound burst of intracellular ROS and H_2O_2 (Figures 2 and 3). These elevated ROS levels then act as potent secondary messengers that cross-talk with and stimulate the redox-sensitive Ras/Raf/MEK/ERK pathway, a progression that is well-supported by our finding that pharmacological NOX2 inhibition via GSK2795039 effectively dampens downstream mitochondrial depolarization. By suppressing NOX2 activation, THC successfully truncates this signaling cascade at its inception, preventing the subsequent downstream activation

of Ras/Raf/MEK/ERK and ultimately preserving RPE cell viability (as schematically summarized in Figure 8).

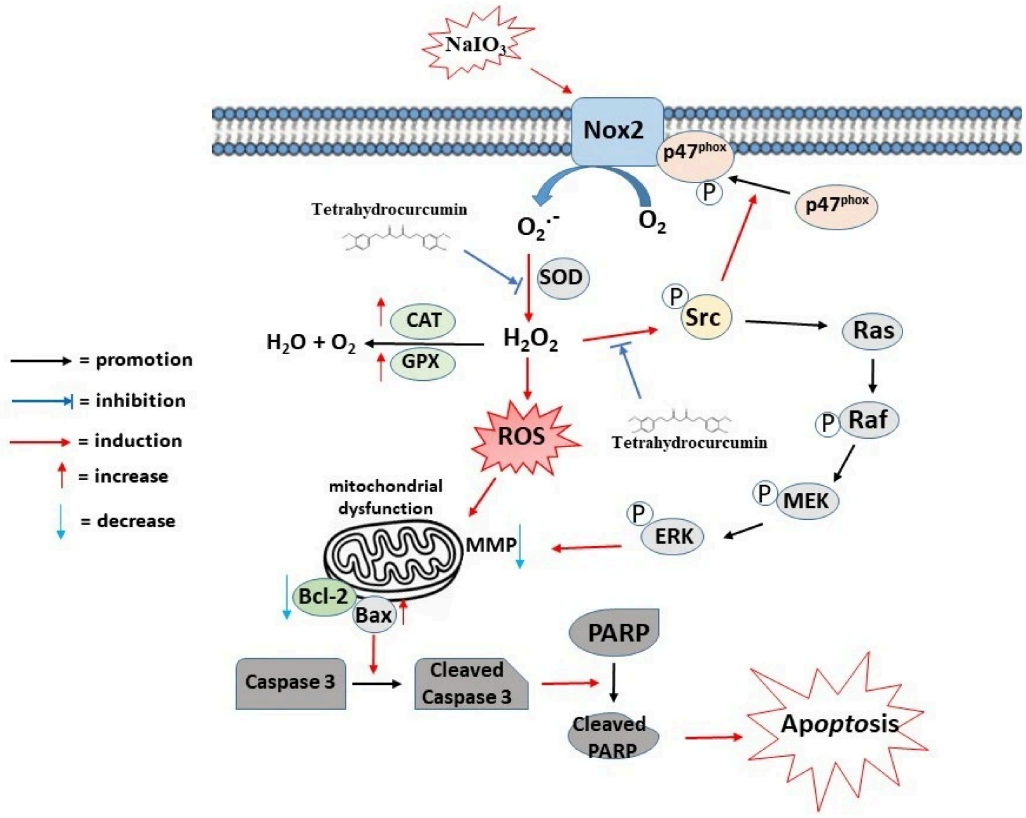

Figure 8. Proposed mechanism underlying the protective effects of tetrahydrocurcumin (THC) against $NaIO_3$-induced oxidative damage in retinal pigment epithelial cells. THC suppresses $NaIO_3$-induced NOX2 activation and ROS generation through inhibition of the Src/$p47^{phox}$/NOX2 signaling pathway, thereby reducing oxidative stress and H_2O_2 accumulation. Consequently, THC preserves mitochondrial membrane potential, attenuates mitochondrial dysfunction, and suppresses apoptosis-associated protein activation, including Bax, cleaved caspase-3, and cleaved PARP. In addition, THC inhibits activation of the Ras/Raf/MEK/ERK signaling cascade, ultimately protecting ARPE-19 cells from oxidative stress-induced apoptosis and retinal degeneration.

It is worth noting that while both autophagy and apoptosis are intricate components of the cellular stress response in RPE degeneration, their precise roles often depend on the intensity and duration of the oxidative stimulus. Accumulating evidence from numerous scholars has previously demonstrated that autophagy typically functions as an early, adaptive, pro-survival mechanism aimed at mitigating mild oxidative damage through the clearance of damaged organelles [50]. However, under severe, acute, or sustained chemical insult—such as the specific dosage of $NaIO_3$ employed in this study—this protective autophagic capacity is frequently overwhelmed or its autophagic flux disrupted, eventually triggering a molecular cross-talk that shifts the cellular equilibrium toward programmed cell death [51,52].

Because our phenotypic characterization and Western blot analyses consistently identified a robust and predominant induction of classic, terminal apoptotic markers (including increased Annexin V-positive populations, Bax upregulation, and the distinct cleavage of caspase-3 and PARP), we focused our mechanistic elucidation primarily on the apoptotic cascade. This allows us to directly trace how THC effectively rescues ARPE-19 cells from terminal oxidative execution without confounding systemic variables. Consequently, THC successfully attenuated the expression of pro-apoptotic proteins (such as Bax, the cleaved

form of caspase-3, and cleaved-PARP) while restoring the levels of the anti-apoptotic protein Bcl-2 in $NaIO_3$-induced ARPE-19 cells (Figure 5B). These findings suggest that THC-mediated retinal protection is at least partially associated with the suppression of oxidative stress-dependent Ras/Raf/MEK/ERK activation and subsequent mitochondrial apoptotic signaling.

In this study, a $NaIO_3$-induced mouse model was employed to determine whether THC could protect against retinal degeneration *in vivo*. Consistent with previous reports, $NaIO_3$ treatment induced marked retinal structural alterations, including photoreceptor IS/OS loss, and ONL thinning and disorganization, indicating successful establishment of a retinal degeneration model [6,46,49]. Notably, daily administration of THC significantly attenuated these pathological changes, suggesting a protective effect against $NaIO_3$-induced retinal injury (Figure 7A). This protective effect may be associated with the suppression of apoptosis, as THC markedly reduced cleaved caspase-3 expression in retinal tissues compared with the $NaIO_3$-treated group (Figure 7C). This was confirmed by pupillary response testing of mice; THC indeed restored normal pupillary responses in $NaIO_3$-treated mice (Figure 7B).

In conclusion, this study demonstrates that THC protects against $NaIO_3$-induced retinal degeneration both *in vitro* and *in vivo*. Mechanistically, THC attenuated oxidative stress, preserved mitochondrial function, suppressed apoptotic signaling, and improved retinal structure and function. These protective effects were associated with inhibition of NOX2-mediated ROS generation and suppression of the Ras/Raf/MEK/ERK signaling pathway, highlighting THC as a promising therapeutic candidate for oxidative stress-related retinal disorders (Figure 8).

5. Conclusions

In summary, the present study demonstrates that THC exerts powerful cytoprotective and histological rescue effects against $NaIO_3$-induced retinal degeneration across both *in vitro* and *in vivo* experimental models. Mechanistically, our findings successfully map a unified, hierarchical signaling network driving RPE cell death: $NaIO_3$ exposure initiates an upstream oxidative cascade governed by the activation of the Src/$p47^{phox}$/NOX2 complex, and the resulting robust burst of intracellular ROS and H_2O_2 acts as a critical secondary messenger axis that cross-talks with and drives the downstream, redox-sensitive Ras/Raf/MEK/ERK pro-apoptotic pathway.

Crucially, pharmacological intervention with THC successfully intercepts this degenerative cascade at its inception by suppressing upstream NOX2 activation, which in turn mitigates severe oxidative injury, preserves mitochondrial membrane potential, and prevents downstream apoptotic execution. Furthermore, our *in vivo* findings translate these molecular mechanisms into physiological outcomes, confirming that daily systemic administration of THC effectively mitigates outer retinal structural atrophy, maintains outer nuclear layer integrity, and preserves visual reflex function as verified by pupillary light responses. Taken together, these convergent lines of evidence validate the targeted therapeutic efficacy of THC, highlighting its clinical potential as a promising pharmacological candidate for the prevention and treatment of dry age-related macular degeneration (dry AMD) and other oxidative stress-driven geographic retinopathies.

Author Contributions: T.-C.C. and T.-L.-T.V.: Writing—original draft, Validation, Project Investigation, Data curation. S.-C.T.: methodology, validation, Data curation. C.-J.C., H.-M.D.W. and I.W.: Writing—review and editing. Y.-Y.C. and H.-W.L.: Writing—review and editing, Supervision, Project administration, Funding acquisition. All authors have read and agreed to the published version of the manuscript.

Funding: This work was financially supported by the National Science and Technology council, Taiwan (project numbers: NSTC 111-2320-B-040-006-MY3 and NSTC 114-2320-B-040-003-MY3). This study was also supported by Chung Shan Medical University and National Chung Hsing University (NCHU-CSMU 11210).

Institutional Review Board Statement: All animal use protocols in this study were approved by the Institutional Animal Care and Use Committee at Chung Shan Medical University (IACUC approval number: 2680; approval date: 23 February 2022), and all investigations were conducted by following the Guide to the Care and Use of Experimental Animals.

Informed Consent Statement: Not applicable.

Data Availability Statement: The original contributions presented in this study are included in the article. Further inquiries can be directed to the corresponding authors.

Acknowledgments: We also thank the Instrument Resource Centre of Chung Shan Medical University for its technical support.

Conflicts of Interest: The authors have no conflicts of interest to declare.

References

1. Guymer, R.H.; Campbell, T.G. Age-related macular degeneration. *Lancet* **2023**, *401*, 1459–1472. [CrossRef]
2. Fleckenstein, M.; Schmitz-Valckenberg, S.; Chakravarthy, U. Age-related macular degeneration: A review. *JAMA* **2024**, *331*, 147–157. [CrossRef]
3. Jiang, B.C.; Wei, X.; Cai, D.M.; Wang, X.; Zhou, X.; Chen, F.; Shen, X.; Cao, X.; Zheng, C. Association between dietary consumption of fatty acids and age-related macular degeneration in the National Health and Nutrition Examination Survey. *Sci. Rep.* **2024**, *14*, 11016. [CrossRef]
4. Tisi, A.; Feligioni, M.; Passacantando, M.; Ciancaglini, M.; Maccarone, R. The impact of oxidative stress on blood-retinal barrier physiology in age-related macular degeneration. *Cells* **2021**, *10*, 64. [CrossRef] [PubMed]
5. Lin, C.C.; Chiu, C.C.; Lee, P.Y.; Chen, K.J.; He, C.X.; Hsu, S.K.; Cheng, K.C. The adverse effects of air pollution on the eye: A review. *Int. J. Environ. Res. Public Health* **2022**, *19*, 1186. [CrossRef] [PubMed]
6. Chang, Y.Y.; Wang, M.L.; Yeh, J.H.; Tsou, S.C.; Chen, T.C.; Hsu, M.Y.; Lee, Y.J.; Wang, I.; Lin, H.W. The protective effects of beta-mangostin against sodium iodate-induced retinal ROS-mediated apoptosis through MEK/ERK and p53 signaling pathways. *Food Funct.* **2023**, *14*, 10896–10909. [CrossRef]
7. Tsou, S.C.; Chuang, C.J.; Wang, I.; Chen, T.C.; Yeh, J.H.; Hsu, C.L.; Hung, Y.C.; Lee, M.C.; Chang, Y.Y.; Lin, H.W. Lemon peel water extract: A novel material for retinal health, protecting retinal pigment epithelial cells against dynamin-related protein 1-mediated mitochondrial fission by blocking ROS-stimulated mitogen-activated protein kinase/extracellular signal-regulated kinase pathway. *Antioxidants* **2024**, *13*, 538.
8. Chen, Y.A.; Lu, W.N.; Li, P.; Nie, T.; Li, Y.; Zeng, R.; Lin, S.; Gao, M.; Hejtmancik, J.F.; Hou, L.; et al. MITF promotes MFN2-dependent mitochondrial fusion to protect retinal pigment epithelial cells from mitochondrial damage. *Free Radic. Biol. Med.* **2025**, *239*, 27–42. [CrossRef] [PubMed]
9. Di Rienzo, M.; Romagnoli, A.; Refolo, G.; Vescovo, T.; Ciccosanti, F.; Zuchegna, C.; Lozzi, F.; Occhigrossi, L.; Piacentini, M.; Fimia, G.M. Role of AMBRA1 in mitophagy regulation: Emerging evidence in aging-related diseases. *Autophagy* **2024**, *20*, 2602–2615. [CrossRef]
10. Fan, X.; Yang, Y.; Wu, G.; Kong, Y.; Zhang, Y.; Zha, X. Circ-CARD6 inhibits oxidative stress-induced apoptosis and autophagy in ARPE-19 cells via the miR-29b-3p/PRDX6/PI3K/Akt axis. *Exp. Eye Res.* **2024**, *238*, 109690, Erratum in *Exp. Eye Res.* **2025**, *259*, 110560. [CrossRef]
11. Sumimoto, H. Structure, regulation and evolution of Nox-family NADPH oxidases that produce reactive oxygen species. *FEBS J.* **2008**, *275*, 3249–3277. [CrossRef] [PubMed]
12. Leto, T.L.; Morand, S.; Hurt, D.; Ueyama, T. Targeting and regulation of reactive oxygen species generation by Nox family NADPH oxidases. *Antioxid. Redox Signal.* **2009**, *11*, 2607–2619. [CrossRef]
13. Vo, T.T.T.; Wee, Y.; Cheng, H.C.; Wu, C.Z.; Chen, Y.L.; Tuan, V.P.; Liu, J.F.; Lin, W.N.; Lee, I.T. Surfactin induces autophagy, apoptosis, and cell cycle arrest in human oral squamous cell carcinoma. *Oral Dis.* **2023**, *29*, 528–541. [CrossRef]
14. Lin, W.Y.; Cheng, Y.H.; Liu, P.Y.; Hsu, S.P.; Lin, S.C.; Chien, C.T. Carvedilol through ß1-Adrenoceptor blockade ameliorates glomerulonephritis via inhibition of oxidative stress, apoptosis, autophagy, ferroptosis, endoplasmic reticulum stress and inflammation. *Biochem. Pharmacol.* **2024**, *230*, 116570. [CrossRef]

15. Matono, R.; Miyano, K.; Kiyohara, T.; Sumimoto, H. Arachidonic acid induces direct interaction of the p67(phox)-Rac complex with the phagocyte oxidase NOX2, leading to superoxide production. *J. Biol. Chem.* **2014**, *289*, 24874–24884. [CrossRef] [PubMed]
16. Knock, G.A. NADPH oxidase in the vasculature: Expression, regulation and signalling pathways; role in normal cardiovascular physiology and its dysregulation in hypertension. *Free Radic. Biol. Med.* **2019**, *145*, 385–427. [CrossRef]
17. Treuer, A.V.; Faúndez, M.; Ebensperger, R.; Hovelmeyer, E.; Vergara-Jaque, A.; Perera-Sardiña, Y.; Gutierrez, M.; Fuentealba, R.; González, D.R. New NADPH oxidase 2 inhibitors display potent activity against oxidative stress by targeting p22(phox)-p47(phox) interactions. *Antioxidants* **2023**, *12*, 1441. [CrossRef]
18. Malaviya, P.; Kumar, J.; Kowluru, R.A. Role of ferroptosis in mitochondrial damage in diabetic retinopathy. *Free Radic. Biol. Med.* **2024**, *225*, 821–832. [CrossRef]
19. Chuang, C.-J.; Wang, M.; Yeh, J.-H.; Chen, T.-C.; Tsou, S.-C.; Lee, Y.-J.; Chang, Y.-Y.; Lin, H.-W. The protective effects of α-mangostin attenuate sodium iodate-induced cytotoxicity and oxidative injury via mediating SIRT-3 inactivation via the PI3K/AKT/PGC-1α pathway. *Antioxidants* **2021**, *10*, 1870. [CrossRef] [PubMed]
20. Lin, H.W.; Chen, T.C.; Yeh, J.H.; Tsou, S.C.; Wang, I.; Shen, T.J.; Chuang, C.J.; Chang, Y.Y. Suppressive effect of tetrahydrocurcumin on *Pseudomonas aeruginosa* lipopolysaccharide-induced inflammation by suppressing JAK/STAT and Nrf2/HO-1 pathways in microglial cells. *Oxid. Med. Cell. Longev.* **2022**, *2022*, 4978556. [CrossRef]
21. Zhou, M.; Li, R.; Hua, H.; Dai, Y.; Yin, Z.; Li, L.; Zeng, J.; Yang, M.; Zhao, J.; Tan, R. The role of tetrahydrocurcumin in disease prevention and treatment. *Food Funct.* **2024**, *15*, 6798–6824. [CrossRef]
22. Park, C.H.; Song, J.H.; Kim, S.N.; Lee, J.H.; Lee, H.J.; Kang, K.S.; Lim, H.H. Neuroprotective effects of tetrahydrocurcumin against glutamate-induced oxidative stress in hippocampal HT22 cells. *Molecules* **2019**, *25*, 144. [CrossRef]
23. Kim, J.E.; Kim, H.R.; Kim, J.C.; Lee, E.S.; Chung, C.H.; Lee, E.Y.; Chung, B.Y. Tetrahydrocurcumin ameliorates skin inflammation by modulating autophagy in high-fat diet-induced obese mice. *BioMed Res. Int.* **2021**, *2021*, 6621027. [CrossRef]
24. Lv, X.; Liu, Z.; Xu, L.; Song, E.; Song, Y. Tetrachlorobenzoquinone exhibits immunotoxicity by inducing neutrophil extracellular traps through a mechanism involving ROS-JNK-NOX2 positive feedback loop. *Environ. Pollut.* **2021**, *268*, 115921. [CrossRef] [PubMed]
25. Zhan, Y.; Chen, Q.; Song, Y.; Wei, X.; Zhao, T.; Chen, B.; Li, C.; Zhang, W.; Jiang, Y.; Tan, Y.; et al. Berbamine hydrochloride inhibits lysosomal acidification by activating NOX2 to potentiate chemotherapy-induced apoptosis via the ROS-MAPK pathway in human lung carcinoma cells. *Cell Biol. Toxicol.* **2023**, *39*, 1297–1317. [CrossRef] [PubMed]
26. Wen, C.; Yu, X.; Zhu, J.; Zeng, J.; Kuang, X.; Zhang, Y.; Tang, S.; Zhang, Q.; Yan, J.; Shen, H. Gastrodin ameliorates oxidative stress-induced RPE damage by facilitating autophagy and phagocytosis through PPARalpha-TFEB/CD36 signal pathway. *Free Radic. Biol. Med.* **2024**, *224*, 103–116. [CrossRef] [PubMed]
27. Hsu, M.Y.; Hsiao, Y.P.; Lin, Y.T.; Chen, C.; Lee, C.M.; Liao, W.C.; Tsou, S.C.; Lin, H.W.; Chang, Y.Y. Quercetin alleviates the accumulation of superoxide in sodium iodate-induced retinal autophagy by regulating mitochondrial reactive oxygen species homeostasis through enhanced deacetyl-SOD2 via the Nrf2-PGC-1α-Sirt1 pathway. *Antioxidants* **2021**, *10*, 1125. [CrossRef]
28. Gaskin, J.C.F.; Shah, M.H.; Chan, E.C. Oxidative stress and the role of NADPH oxidase in glaucoma. *Antioxidants* **2021**, *10*, 238. [CrossRef]
29. Feng, Y.; Wang, X.; Li, P.; Shi, X.; Prokosch, V.; Liu, H. Exogenous hydrogen sulfide and NOX2 inhibition mitigate ferroptosis in pressure-induced retinal ganglion cell damage. *Biochim. Biophys. Acta Mol. Basis Dis.* **2025**, *1871*, 167705. [CrossRef]
30. Chowdhury, A.K.; Watkins, T.; Parinandi, N.L.; Saatian, B.; Kleinberg, M.E.; Usatyuk, P.V.; Natarajan, V. Src-mediated tyrosine phosphorylation of $p47^{phox}$ in hyperoxia-induced activation of NADPH oxidase and generation of reactive oxygen species in lung endothelial cells. *J. Biol. Chem.* **2005**, *280*, 20700–20711. [CrossRef]
31. Sato, Y.; Fujimoto, S.; Mukai, E.; Sato, H.; Tahara, Y.; Ogura, K.; Yamano, G.; Ogura, M.; Nagashima, K.; Inagaki, N. Palmitate induces reactive oxygen species production and beta-cell dysfunction by activating nicotinamide adenine dinucleotide phosphate oxidase through Src signaling. *J. Diabetes Investig.* **2014**, *5*, 19–26. [CrossRef] [PubMed]
32. Jarrett, S.G.; Boulton, M.E. Consequences of oxidative stress in age-related macular degeneration. *Mol. Asp. Med.* **2012**, *33*, 399–417. [CrossRef]
33. Zou, G.P.; Wang, T.; Xiao, J.X.; Wang, X.Y.; Jiang, L.P.; Tou, F.F.; Chen, Z.P.; Qu, X.H.; Han, X.J. Lactate protects against oxidative stress-induced retinal degeneration by activating autophagy. *Free Radic. Biol. Med.* **2023**, *194*, 209–219. [CrossRef]
34. Liu, J.; Han, X.; Zhang, T.; Tian, K.; Li, Z.; Luo, F. Reactive oxygen species (ROS) scavenging biomaterials for anti-inflammatory diseases: From mechanism to therapy. *J. Hematol. Oncol.* **2023**, *16*, 116. [CrossRef]
35. Koklesova, L.; Liskova, A.; Samec, M.; Zhai, K.; Al-Ishaq, R.K.; Bugos, O.; Šudomová, M.; Biringer, K.; Pec, M.; Adamkov, M.; et al. Protective effects of flavonoids against mitochondriopathies and associated pathologies: Focus on the predictive approach and personalized prevention. *Int. J. Mol. Sci.* **2021**, *22*, 8649. [CrossRef]
36. Kowluru, R.A.; Kowluru, A.; Veluthakal, R.; Mohammad, G.; Syed, I.; Santos, J.M.; Mishra, M. TIAM1-RAC1 signalling axis-mediated activation of NADPH oxidase-2 initiates mitochondrial damage in the development of diabetic retinopathy. *Diabetologia* **2014**, *57*, 1047–1056. [CrossRef]

37. Hou, L.; Wang, K.; Zhang, C.; Sun, F.; Che, Y.; Zhao, X.; Zhang, D.; Li, H.; Wang, Q. Complement receptor 3 mediates NADPH oxidase activation and dopaminergic neurodegeneration through a Src-Erk-dependent pathway. *Redox Biol.* **2018**, *14*, 250–260, Erratum in *Redox Biol.* **2024**, *78*, 103429. [CrossRef]
38. Hernandes, M.S.; Xu, Q.; Griendling, K.K. Role of NADPH Oxidases in blood-brain barrier disruption and ischemic stroke. *Antioxidants* **2022**, *11*, 1966. [CrossRef] [PubMed]
39. Lee, Y.J.; Cho, H.N.; Jeoung, D.I.; Soh, J.W.; Cho, C.K.; Bae, S.; Chung, H.Y.; Lee, S.J.; Lee, Y.S. HSP25 overexpression attenuates oxidative stress-induced apoptosis: Roles of ERK1/2 signaling and manganese superoxide dismutase. *Free Radic. Biol. Med.* **2004**, *36*, 429–444. [CrossRef] [PubMed]
40. Contreras, E.O.; Dearing, C.G.; Ashinhurst, C.A.; Fish, B.A.; Hossain, S.N.; Rey, A.M.; Silva, P.D.; Thompson, S. Pupillary reflex and behavioral masking responses to light as functional measures of retinal degeneration in mice. *PLoS ONE* **2021**, *16*, e0244702. [CrossRef]
41. Yang, Y.C.; Chien, Y.; Yarmishyn, A.A.; Lim, L.Y.; Tsai, H.Y.; Kuo, W.C.; Tsai, P.H.; Yang, S.H.; Hong, S.I.; Chen, S.J.; et al. Inhibition of oxidative stress-induced epithelial-mesenchymal transition in retinal pigment epithelial cells of age-related macular degeneration model by suppressing ERK activation. *J. Adv. Res.* **2024**, *60*, 141–157. [CrossRef]
42. Liu, K.; Li, Y.; Zhong, X.; Hou, Y.; Fei, S.; Chen, E.; Tan, M. Protection effect of lutein-loaded pickering emulsion prepared via ultrasound-assisted Maillard reaction conjugates on dry age-related macular degeneration. *Food Funct.* **2024**, *15*, 6347–6358. [CrossRef]
43. Chan, E.C.; van Wijngaarden, P.; Liu, G.S.; Jiang, F.; Peshavariya, H.; Dusting, G.J. Involvement of NOX2 NADPH Oxidase in retinal neovascularization. *Investig. Ophthalmol. Vis. Sci.* **2013**, *54*, 7061–7067. [CrossRef]
44. Peng, J.J.; Xiong, S.Q.; Ding, L.X.; Peng, J.; Xia, X.B. Diabetic retinopathy: Focus on NADPH oxidase and its potential as therapeutic target. *Eur. J. Pharmacol.* **2019**, *853*, 381–387. [CrossRef]
45. Dionysopoulou, S.; Wikstrom, P.; Bucolo, C.; Romano, G.L.; Micale, V.; Svensson, R.; Spyridakos, D.; Mastrodimou, N.; Georgakis, S.; Verginis, P.; et al. Topically administered NOX4 Inhibitor, GLX7013114, is efficacious in treating the early pathological events of diabetic retinopathy. *Diabetes* **2023**, *72*, 638–652. [CrossRef]
46. Tsou, S.C.; Chuang, C.J.; Hsu, C.L.; Chen, T.C.; Yeh, J.H.; Wang, M.; Wang, I.; Chang, Y.Y.; Lin, H.W. The novel application of EUK-134 in retinal degeneration: Preventing mitochondrial oxidative stress-triggered retinal pigment epithelial cell apoptosis by suppressing MAPK/p53 signaling pathway. *Environ. Toxicol.* **2025**, *40*, 88–100. [CrossRef]
47. Asati, V.; Mahapatra, D.K.; Bharti, S.K. PI3K/Akt/mTOR and Ras/Raf/MEK/ERK signaling pathways inhibitors as anticancer agents: Structural and pharmacological perspectives. *Eur. J. Med. Chem.* **2016**, *109*, 314. [CrossRef]
48. Moustardas, P.; Aberdam, D.; Lagali, N. MAPK pathways in ocular pathophysiology: Potential therapeutic drugs and challenges. *Cells* **2023**, *12*, 617. [CrossRef] [PubMed]
49. Abdelmoaty, A.A.; Zhang, P.; Lin, W.; Fan, Y.J.; Ye, S.N.; Xu, J.H. C0818, a novel curcumin derivative, induces ROS-dependent cytotoxicity in human hepatocellular carcinoma cells *in vitro* via disruption of Hsp90 function. *Acta Pharmacol. Sin.* **2022**, *43*, 446–456. [CrossRef] [PubMed]
50. Chan, C.M.; Huang, D.Y.; Sekar, P.; Hsu, S.H.; Lin, W.W. Reactive oxygen species-dependent mitochondrial dynamics and autophagy confer protective effects in retinal pigment epithelial cells against sodium iodate-induced cell death. *J. Biomed. Sci.* **2019**, *26*, 40, Erratum in *J. Biomed. Sci.* **2019**, *26*, 66. [CrossRef] [PubMed]
51. Dorion, M.F.; Mulumba, M.; Kasai, S.; Itoh, K.; Lubell, W.D.; Ong, H. The CD36 ligand-promoted autophagy protects retinal pigment epithelial cells from oxidative stress. *Oxid. Med. Cell. Longev.* **2021**, *2021*, 6691402. [CrossRef]
52. Tsai, H.Y.; Lai, H.I.A.M.; Chen, Z.Y.; Lin, T.C.; Khor, W.; Kuo, W.C.; Syu, J.P.; Tsai, P.H.; Yang, Y.P.; Chen, Y.; et al. Inhibition of DUSP6 activates autophagy and rescues the retinal pigment epithelium in sodium iodate-induced retinal degeneration models *in vivo* and *in vitro*. *Biomedicines* **2022**, *10*, 159. [CrossRef]

Disclaimer/Publisher's Note: The statements, opinions and data contained in all publications are solely those of the individual author(s) and contributor(s) and not of MDPI and/or the editor(s). MDPI and/or the editor(s) disclaim responsibility for any injury to people or property resulting from any ideas, methods, instructions or products referred to in the content.